The interaction between lipids and ammoniacal nitrogen mitigates inhibition in mesophilic anaerobic digestion

Sergi Astals, Juan José Chávez-Fuentes, Gabriel Capson-Tojo, Miroslav Hutňan, Paul D Jensen

Waste Management 136 (2021) 244–252

Contents lists available at ScienceDirect

Waste Management

journal homepage: www.elsevier.com/locate/wasman

The interaction between lipids and ammoniacal nitrogen mitigates inhibition in mesophilic anaerobic digestion

Sergi Astals [a,b,*], Juan José Chávez-Fuentes [c], Gabriel Capson-Tojo [a,d], Miroslav Hutňan [c], Paul D. Jensen [a]

[a] Advanced Water Management Centre, The University of Queensland, QLD 4072, Australia
[b] Department of Chemical Engineering and Analytical Chemistry, University of Barcelona, 08028 Barcelona, Spain
[c] Institute of Chemical and Environmental Engineering, Slovak University of Technology in Bratislava, 81237 Bratislava, Slovakia
[d] CRETUS, Department of Chemical Engineering, Universidade de Santiago de Compostela, 15782 Santiago de Compostela, Galicia, Spain

ARTICLE INFO

Keywords:
Anaerobic digestion
Anaerobic co-digestion
Slaughterhouse waste
Modelling
Ammonia nitrogen
Long chain fatty acids

ABSTRACT

Ammoniacal nitrogen and long chain fatty acids (LCFA) are common inhibitors of the anaerobic digestion process. However, the interaction between these inhibitors has received little attention. Understanding the interaction between these inhibitors is important to optimise the operation of anaerobic digesters treating slaughterhouse waste or using fat, oil and grease (FOG) as co-substrate among others. To study the interaction between ammoniacal nitrogen and LCFA inhibition, 20 different conditions were trialled in mesophilic batch tests. Experimental conditions included 5 mixtures between slaughterhouse wastewater and LCFA (100:0, 75:25, 50:50, 20:80, 0:100 on a VS basis), each one tested at 4 different ammoniacal nitrogen concentrations (0, 1, 3, 6 $gN_{added}·L^{-1}$). Experimental and modelling results showed that ammoniacal nitrogen inhibition was less severe in LCFA-rich mixtures, indicating that LCFA mitigated ammoniacal nitrogen inhibition to a certain extent. However, the positive interaction between inhibitors did not only depend on the LCFA concentration. A protective LCFA coat that limited the diffusion of free ammonia into the cell and/or provided a localised lower pH in the vicinity of the microbial cell could explain the experimental results. However, ammoniacal nitrogen and LCFA inhibition comprise up to 6 different but interrelated inhibitors (i.e. NH_3, NH_4^+, LCFA, VFA, H_2 and pH) and therefore the specific mechanism could not be elucidated. Nonetheless, these results suggest that LCFA do not exacerbate TAN-related inhibition and that LCFA-rich substrates can be utilised as co-substrates in mesophilic N-rich digesters.

1. Introduction

Anaerobic digestion (AD), a biological process that transforms organic matter into biogas, is a commercial reality used to treat several organic waste streams (Mao et al., 2015). However, single substrates AD (mono-digestion) can present challenges related to the intrinsic properties of the substrate, which can lead to poor biogas yields and instability events (Hagos et al., 2017; Mata-Alvarez et al., 2014). For instance, AD of slaughterhouse waste (SHW) may present operational problems linked to the high concentrations of long chain fatty acids (LCFA) and ammoniacal nitrogen, both well-known inhibitors of acetoclastic methanogens (Capson-Tojo et al., 2020; Elsamadony et al., 2021; Palatsi et al., 2011; Rajagopal et al., 2013).

Anaerobic co-digestion (AcoD) is the process where two or more substrates, ideally with complementary characteristics, are mixed for combined treatment. Despite the potential benefits of combining complementarity substrates, in practice, co-substrate selection is primarily based on availability and economic criteria (Mata-Alvarez et al., 2014; Nghiem et al., 2017). Random or heuristic decisions on co–substrate selection and dosage can lead to negative effects on digesters performance (García-Gen et al., 2015a; Xie et al., 2016). Fat, oil and grease (FOG) is amongst the most researched and applied co-substrates. However, most research has focused on boosting biogas production by means of optimising the mixing ratio or by increasing the loading rate, while little attention has been given to the interaction between inhibitors (Hagos et al., 2017; Long et al., 2012; Mata-Alvarez et al., 2014; Xie et al., 2016). AcoD research has overlooked potential synergetic or antagonistic interactions between inhibitors, which can

* Corresponding author.
E-mail address: sastals@ub.edu (S. Astals).

https://doi.org/10.1016/j.wasman.2021.10.015
Received 19 August 2021; Received in revised form 6 October 2021; Accepted 11 October 2021
Available online 23 October 2021

play a significant role in AD performance and stability, and therefore should be considered for co-substrate selection.

Ammoniacal nitrogen (sum of NH_3 and NH_4^+) and LCFA are among the most common inhibitors in AD systems (Capson-Tojo et al., 2020; Chen et al., 2014; Elsamadony et al., 2021). However, they are characterised by completely different inhibition mechanisms. The inhibition mechanism of ammoniacal nitrogen is primarily linked to the capacity of ammonia (NH_3) to diffuse into the microbial cell, causing proton imbalance and potassium deficiency (Kayhanian, 1999; Rajagopal et al., 2013). However, ammoniacal nitrogen inhibition has also been related to high ammonium ion (NH_4^+) concentrations, which may inhibit methane-synthesising enzymes (Astals et al., 2018; Lay et al., 1998; Yenigün and Demirel, 2013). Co-digestion studies for N-rich AD systems (mostly animal manure or food waste) primarily aim to balance total ammoniacal nitrogen (TAN) concentration by adding a carbon-rich substrate such as crop wastes, paper/cardboard waste and crude glycerol (Hagos et al., 2017; Mata-Alvarez et al., 2014; Xie et al., 2016). Lipid-rich waste streams such as grease trap waste, oil mill wastes, and dissolved-air flotation sludge are also very attractive co-substrates for N-rich digesters, since they are carbon-rich and have high methane yields (>600 $mLCH_4 \cdot gVS^{-1}$) (Long et al., 2012; Salama et al., 2019). Nonetheless, lipid dosage needs to be managed to avoid inhibition by LCFA (Elsamadony et al., 2021; Long et al., 2012). The inhibitory mechanism of LCFA is associated with their capacity to be adsorbed onto the microbial cell membrane, forming a barrier that disrupts membrane functionality and limits the transfer of substrates and products (Pereira et al., 2005; Rasit et al., 2015; Rodríguez-Méndez et al., 2017).

The inhibitory interaction between ammoniacal nitrogen and LCFA is not well understood, however, it may have a major impact on co-substrate selection and dosage for N-rich AD systems. To date, the few publications addressing this subject have reported conflicting results. Based on a dynamic model, Angelidaki et al. (1999) suggested that the addition of lipids could alleviate NH_3 inhibition as a result of an increased biomass growth. In the model, higher biomass concentrations were required to degrade the additional carbon, where NH_3 inhibition decreased due to inorganic nitrogen uptake for biomass growth. However, Wang et al. (2016) calculated that biomass growth only uptakes 23 mg of ammoniacal nitrogen per gram of lipid degraded. Thus, the impact of biomass growth on the NH_3 concentration is negligible. Besides, Wang et al. (2016) reported a negative interaction between ammoniacal nitrogen and lipids, when the ammoniacal nitrogen concentration in a thermophilic digester fed with cattle manure and glycerol trioleate was increased from 4 to 5 $gTAN \cdot L^{-1}$. In a subsequent study by the same research group, Tian et al. (2018) hypothesised that the negative interaction between ammoniacal nitrogen and LCFA was caused by the inhibition of methanogens by NH_3, which increased the H_2 concentration and made LCFA β-oxidation less thermodynamically favourable. This hypothesis was supported by thermophilic batch and continuous experiments. Contrariwise, Fernandes et al. (2012) reported no impact of ammoniacal nitrogen concentration (up to 7.8 $gTAN \cdot L^{-1}$) on the degradation kinetics of tributyrin under mesophilic conditions. However, tributyrin is more easily hydrolysable than LCFA, and therefore it is expected to be less inhibitory than LCFA (Fernandes et al., 2012). While Tian et al. (2018) analysed the interaction between ammoniacal nitrogen and LCFA under thermophilic conditions (theoretically more prone to ammonia and LCFA inhibition), no systematic research has been conducted under mesophilic conditions. It is important to state that thermophilic results cannot be extrapolated to mesophilic conditions since temperature plays a significant impact on LCFA solubility and on ammoniacal nitrogen fractionation, which can have a strong impact on the observed response.

The goal of this work was to study the interaction between ammoniacal nitrogen and LCFA in mesophilic anaerobic digestion. To achieve this goal, wastewater from a cattle slaughterhouse was used as a base substrate due to (i) its high protein content and (ii) the relevance of this research to slaughterhouse AD applications. The cattle slaughterhouse wastewater was co-digested with LCFA at different ammoniacal nitrogen concentrations. Specifically, 20 different conditions were tested in batch tests, comprising 5 mixtures of slaughterhouse wastewater and LCFA, each of them at 4 different ammoniacal nitrogen concentrations. To gain further insight, the experimental results were also analysed using a mathematical model.

2. Materials and Methods

2.1. Substrates, inoculum and chemicals source

The slaughterhouse wastewater used in this study was collected from a cattle-only slaughterhouse in New South Wales (Australia). The wastewater (so-called red stream (RS)) was a mixture of wastewaters from the slaughter floor and rendering areas of the slaughterhouse, which was pre-treated using a dissolved-air flotation (DAF) unit to reduce its lipid content. Extra-virgin olive oil (Carbonell S.A., Spain) was used as a source of LCFA. Olive oil mainly contains oleic, linoleic and palmitic acids (Orsavova et al., 2015). Ammonium chloride (Merck KGaA, Germany) was used as external source of ammoniacal nitrogen. The inoculum was collected from the bottom layer (~3 m) of an anaerobic lagoon located at the aforementioned slaughterhouse. The anaerobic lagoon treats a mix of wastewater from the slaughterhouse after its pre-treatment to reduce its coarse solids and lipid content. The composition of the RS and the inoculum is shown in Table 1. A more detailed characterisation is provided in Table S1 in the supplementary material.

2.2. Anaerobic batch tests

Mesophilic batch tests were carried out in 310 mL serum bottles following Angelidaki et al. (2009) and Holliger et al. (2016). The tests contained inoculum, the amount of substrate (RS) and/or co-substrate (olive oil) needed to obtain the desired mixture, and the amount of ammonium chloride needed to reach a specific TAN concentration. All tests had an inoculum-to-substrate ratio (ISR) of 2 on a VS basis. No external buffers or trace elements were added. The pH of each bottle was measured after adding all the reagents (the pH was never adjusted). A blank assay containing only inoculum was used to correct the background methane production from the inoculum endogenous respiration. The headspace of each bottle was flushed with 99.99 % N_2 gas for 1 min (4 $L \cdot min^{-1}$). The bottles were sealed with a rubber stopper, retained with an aluminium crimp seal and stored in an incubator at 37 ± 1 °C. At each sampling event, the biogas volume and composition (CH_4, CO_2 and H_2) were measured using a bench-top manometer and a gas chromatograph, respectively. The tests were mixed by swirling before each sampling event. Cumulative volumetric gas production was calculated from the pressure increase in the headspace volume and expressed under standard conditions (0 °C, 1 atm, dry). The test with oleic acid and inoculum was also used as a positive control. All tests were carried out until the daily net methane production was lower than 1% of the

Table 1
Characteristics of the red stream and the inoculum. Errors represent the 95% confidence interval in the mean value (n = 3).

Parameter	Units	Red stream	Inoculum
pH	–	6.5 ± 0.1	7.1 ± 0.1
TS	$g \cdot L^{-1}$	6.2 ± 0.1	18.6 ± 0.1
VS	$g \cdot L^{-1}$	5.7 ± 0.1	13.9 ± 0.1
TCOD	$gO_2 \cdot L^{-1}$	10.6 ± 0.8	22.0 ± 2.3
sCOD	$gO_2 \cdot L^{-1}$	5.5 ± 0.2	0.2 ± 0.1
Lipids	$g \cdot L^{-1}$	2.1 ± 0.2	–
VFA	$mg \cdot L^{-1}$	189 ± 11	7 ± 1
TAN	$mgN \cdot L^{-1}$	68 ± 2	282 ± 7
TKN	$mgN \cdot L^{-1}$	232 ± 15	1237 ± 41
PO_4-P	$mgP \cdot L^{-1}$	35 ± 2	34 ± 2

cumulative net methane production for at least 3 consecutive days (Holliger et al., 2016). The TAN concentration and pH of each bottle were measured immediately after the final sampling event. All tests and blanks were carried out in triplicate.

2.3. Experimental design

The experimental design used in this study is summarised in Fig. 1. The experiment consisted of different combinations of RS and olive oil (LCFA source). The experiment included mono-digestion references for RS (0 LCFA/100 RS) and LCFA (100 LCFA/0 RS), and 3 co-digestion mixtures (i.e. 25 LCFA/75 RS, 50 LCFA/50 RS, 80 LCFA/20 RS on a VS basis). This co-digestion mixtures were designed to study a wide range of proportions between both substrates. Each combination was tested at four different ammoniacal nitrogen concentrations: one control with no added TAN (referred as 0 $gTAN_{added}·L^{-1}$) and three additional concentrations where TAN was added to the background concentration, i.e. 1, 3 and 6 $gTAN_{added}·L^{-1}$. TAN concentrations were chosen based on literature values for low, medium and high TAN inhibitory concentrations (Capson-Tojo et al., 2020; Lu et al., 2018; Rajagopal et al., 2013; Yenigün and Demirel, 2013). Therefore, a total of 20 different conditions were tested. Table S2 in the supplementary material provides additional information on the initial and final characteristics of each batch, i.e. added TAN and LCFA concentrations, measured TAN concentrations, pH values, and estimated NH_3 concentrations.

2.4. Analytical methods

Analyses of the total fraction were performed directly on the raw samples. For analyses of the soluble fraction, the samples were centrifuged at 2500 × g for 5 min and the supernatant was filtered through a 0.45 µm PES Millipore® filter. Total solids (TS) and volatile solids (VS) were measured according to Standard Methods 2540G (APHA, 2012). Total (TCOD) and soluble (sCOD) chemical oxygen demand were measured using Merck Spectroquant® test kit and a Move 100 colorimeter (Merck, Germany). pH value was measured with a TPS WP-80D multi-parameter meter equipped with a TPS-121210 micro pH sensor. Volatile fatty acids (VFA, i.e. acetic, propionic, butyric and valeric acid) were analysed with an Agilent 7890A gas chromatograph equipped with an Agilent DB-FFAP column. Lipids were measured as FOG using S316 as extraction solvent and a Wilks InfraCal TOG/TPH analyser. TAN and total Kjeldahl nitrogen (TKN) were determined with a Lachat QuickChem® 8500 flow injection analyser following the manufacturer's protocol. Ammonia concentration ($gNH_3\text{-}N·L^{-1}$) was calculated using equation (1) (Capson-Tojo et al., 2020) where the acid-base equilibrium constant for inorganic nitrogen (K_a) at the assay temperature (37 °C) is $1.27·10^{-9}$. The activity coefficients (γ_1) in equation (1) were calculated

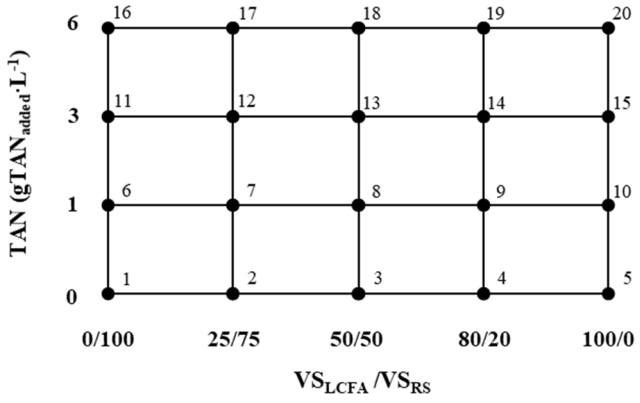

Fig. 1. Experimental design of this study, consisting of 5 different mixtures of red stream (RS) and LCFA, all tested at four different ammoniacal nitrogen (TAN) concentrations.

using the procedure and modified Davies equation suggested by Capson-Tojo et al. (2020) (equation (2)), where ionic strength (I) was calculated considering that the only two contributors were the NH_4^+ and its monovalent counterion.

$$NH_3 - N = \frac{K_a \cdot TAN \cdot \gamma_1}{K_a \cdot \gamma_1 + 10^{-pH}} \quad (1)$$

$$\log\gamma_1 = -0.5 \cdot \left(\frac{\sqrt{I}}{1+\sqrt{I}} - 0.1276 \cdot I \right) \quad (2)$$

Metals were quantified by inductively coupled plasma optical emission spectrometry (ICP-OES) using a Perkin Elmer Optima 7300DV. Biogas composition (CH_4, CO_2, H_2 and N_2) was determined using a Shimadzu GC-2014 equipped with a HAYESEP Q 80/100 packed column and a thermal conductivity detector.

2.5. Mathematical modelling of the methane production curves

The methane production curves were modelled using a first-order kinetic model (equation (3)) (Peces et al., 2020; Zonta et al., 2013). As for Romero-Guiza et al. (2016), model fitting was performed on raw methane production curves prior to blank correction, this approach allowed to model the reduced background methane production in inhibited tests. The methane production from the inoculum was modelled using a two-substrate first-order kinetic model since the one-substrate first-order kinetic model did not properly fit the blank profile. In the two-substrate first-order kinetic model, the substate is split into a rapidly biodegradable and a slowly biodegradable fraction (García-Gen et al., 2015b; Weinrich et al., 2020).

$$r = \sum_i (350 \cdot f_i \cdot k_i \cdot X_i \cdot C_i \cdot I_{LCFA} \cdot I_N) \quad (3)$$

where r is the process rate ($mLCH_4·L^{-1}·day^{-1}$), 350 is the conversion ratio based on the maximum theoretical methane yield at standard conditions ($mLCH_4·gCOD^{-1}$), f_i is the biodegradability of the substrate (-), k_i is the first-order rate constant of the substrate (day^{-1}), X_i is the substrate concentration ($gVS·L^{-1}$), C_i is the COD-to-VS ratio of the substrate, I_{LCFA} is the inhibition factor for LCFA, and I_N is the inhibition factor for ammoniacal nitrogen. Subscript i is either RS, LCFA, inoculum fast fraction or inoculum slow fraction. Note S1 in the supplementary material provides detailed information regarding the model.

Inhibition factors were included to model the impact of LCFA (I_{LCFA}) and ammoniacal nitrogen (I_N) on batch test results. Inhibition factors range from 1 (no inhibition) to 0 (total inhibition). LCFA inhibition was modelled using a threshold inhibition (equation (4)) (Arnell et al., 2016; Peces et al., 2020).

$$I_{LCFA} = \begin{cases} 1 & for [LCFA] \le KI_{lcfa,min} \\ e^{-2.77259 \left(\frac{([LCFA] - KI_{lcfa,min})}{(KI_{lcfa,max} - KI_{lcfa,min})} \right)^2} & for [LCFA] > KI_{lcfa,min} \end{cases} \quad (4)$$

where [LCFA] is the long chain fatty acids concentration ($gVS_{LCFA}·L^{-1}$), $KI_{lcfa,min}$ is the LCFA concentration where inhibition starts (onset concentration), and $KI_{lcfa,max}$ is the LCFA concentration at which the inhibition is almost complete ($I_{LCFA} \approx 0$).

The ammoniacal nitrogen inhibition factor (I_N) was implemented as a correction factor not linked to any physico-chemical property to allow the model to find the I_N value that best fitted the experimental data. This approach was chosen because the implementation of an inhibition function was unable to fit the experimental data, likely because the interaction between ammoniacal nitrogen and LCFA did not allow modelling the experimental results using a single set of inhibition parameters. Furthermore, due to the low NH_3 and NH_4^+ concentrations, it was assumed that I_N was 1 in all the batch tests with no added TAN. The batch test modelling was done following three steps:

1. The blank test was modelled to determine: $f_{inoculum,fast}$, $f_{inoculum,slow}$, $k_{inoculum,fast}$, $k_{inoculum,slow}$.
2. Using the inoculum parameters, the 5 batch tests with no added TAN were jointly modelled to determine: f_{rs}, f_{lcfa}, k_{rs}, k_{lcfa}, $KI_{lcfa,min}$, $KI_{lcfa,max}$.
3. Using the stoichiometric and kinetic parameters determined in step 1 and 2, the I_N that best fitted the experimental data were individually determined for each of the tests carried out at 1, 3 and 6 $gTAN_{added}·L^{-1}$.

The model was implemented in Aquasim 2.1d. Parameter uncertainty was estimated based on a two-tailed *t*-test on parameter standard error around the optimum, and non-linear confidence regions were also tested to confirm that the linear estimate was representative of true confidence (Jensen et al., 2011). The objective function minimised was the sum of squared errors (χ^2), where average data from triplicate experiments were used as the model target.

3. Results

3.1. Individual LCFA and TAN inhibition

3.1.1. LCFA inhibition

Fig. 2 displays the normalised degradation curves of the tests performed without TAN addition, from which the impact of LCFA addition can be directly assessed. The methane cumulative curves were normalised against the final methane yield to provide a more direct comparison between tests (Fig. S1 in the supplementary material displays the non-normalised curves and their standard deviation). Fig. 2 shows how degradation kinetics decreased as the LCFA content in the mixture increased. This behaviour can be explained by the lower degradation rate of LCFA (0.05 day^{-1}) compared to RS (0.22 day^{-1}) and by the associated LCFA inhibition (Table 2).

3.1.2. TAN inhibition

Fig. 3A and 3E show the cumulative methane production from RS and LCFA mono-digestion tests at 0, 1 and 3 $gTAN_{added}·L^{-1}$, respectively. Fig. 3 does not display the cumulative methane production of the test carried out at 6 $gTAN_{added}·L^{-1}$ since these assays were completely inhibited. From both mono-digestion results, the individual impact of TAN inhibition can be assessed. The addition of 1 $gTAN·L^{-1}$ only had a minor impact on RS and LCFA degradation kinetics compared to the 0 $gTAN_{added}·L^{-1}$. Nonetheless, the addition of 3 $gTAN·L^{-1}$ had a noticeable impact on LCFA degradation kinetics, where the observed first-order degradation kinetics decreased from 0.05 to 0.03 day^{-1}. The addition of 3 $gTAN·L^{-1}$ to RS had a severe impact on test results where no net methane production was recorded for over 50 days (Fig. 3A). The addition of 6 $gTAN·L^{-1}$ completely inhibited both mono-digestion experiments since no net methane production was recorded for over 100 days.

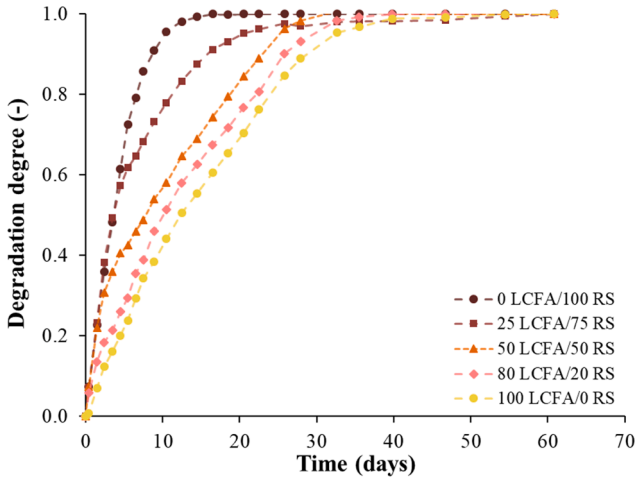

Fig. 2. Normalised degradation curves (as fraction of the final methane yield) of the batch tests performed without TAN addition.

Table 2
Calibrated stoichiometric and kinetic parameters for RS, LCFA and inoculum. Errors represent the 95% confidence interval.

Parameter	Units	
f_{rs}	–	0.85 ± 0.01
f_{lcfa}	–	0.87 ± 0.02
$f_{inoc,fast}$	–	0.04 ± 0.01
$f_{inoc,slow}$	–	0.23 ± 0.02
k_{rs}	day^{-1}	0.22 ± 0.01
k_{lcfa}	day^{-1}	0.050 ± 0.007
$k_{inoculum,fast}$	day^{-1}	0.40 ± 0.01
$k_{inoculum,slow}$	day^{-1}	0.016 ± 0.002
$KI_{lcfa,min}$	$gVS·L^{-1}$	4.1 ± 0.3
$KI_{lcfa,max}$	$gVS·L^{-1}$	15.9 ± 3.2

3.2. Combined LCFA and TAN inhibition

Fig. 3B – 3D show the cumulative methane production from RS and LCFA co-digestion at 0, 1 and 3 $gTAN_{added}·L^{-1}$. The addition of 1 $gTAN·L^{-1}$ had little impact on co-digestion degradation kinetics. Indeed, the degradation kinetics of 25 LCFA/75 RS and 50 LCFA/50 RS were not visibly affected at 1 $gTAN_{added}·L^{-1}$. The addition of 3 $gTAN·L^{-1}$ had a higher impact on the degradation kinetics. TAN inhibition was more severe on the test with lower LCFA content (i.e. 0 LCFA/100 RS and 25 LCFA/75 RS) where no net methane production was recorded for over 50 days (Fig. 3A and 3B). Tests with higher LCFA concentrations did not show such strong inhibition. The 80 LCFA/20 RS was the less inhibited test at 3 $gTAN_{added}·L^{-1}$ followed by the 100 LCFA/0 RS and the 50 LCFA/50 RS tests. The lesser extent of inhibition in the test with higher LCFA content indicates that LCFA may have mitigated TAN inhibition.

Another approach to examine the interaction between LCFA and TAN is to compare experimental and theoretical prediction curves from the co-digestion experiments. Theoretical co-digestion curves are based on the combination of mono-digestion curves (RS and LCFA) at a particular TAN concentration over time and proportioned to the amount of substrate present in the mixture (Fig. 4). The comparison shows that the theoretical and experimental plots at 0 and 1 $gTAN_{added}·L^{-1}$ were quite similar for all mixtures, while at 3 $gTAN_{added}·L^{-1}$ the proportionality was lost. The 25 LCFA/75 RS mixture was more inhibited than expected while the two other mixtures (50 LCFA/50 RS and 80 LCFA/20 RS) were less inhibited than expected. These results reinforce the idea that LCFA alleviated ammoniacal nitrogen inhibition to a certain extent.

3.3. Modelling outputs

Table 2 shows the model stoichiometric and kinetic parameters for RS, LCFA and inoculum. Fig. 5 displays the experimental data and the modelled curves from which stoichiometric and kinetic parameters were obtained (i.e. 0 $gTAN_{added}·L^{-1}$). RS and LCFA biodegradability were high (≥85%). The first-order hydrolysis rate constant for RS was much higher than the one for LCFA (0.22 day^{-1} and 0.05 day^{-1}, respectively). The estimated onset concentration for LCFA inhibition ($KI_{lcfa,min}$) was 4.1 $gVS·L^{-1}$ (~12 $gCOD·L^{-1}$). This indicates that the 80 LCFA/20 RS and the 100 LCFA/0 RS tests were moderately inhibited by LCFA (initial LCFA concentration of 4.8 and 6.9 $gVS·L^{-1}$, respectively; Table S2). The $KI_{lcfa,max}$ was estimated at 15.9 $gVS·L^{-1}$.

Fig. 6 shows the ammoniacal nitrogen inhibition profile of the batch tests, where the TAN inhibition factor (I_N) ranges from 1 (white, no inhibition) to 0 (black, total inhibition).

The I_N factor of each test and the experimental vs. the modelled

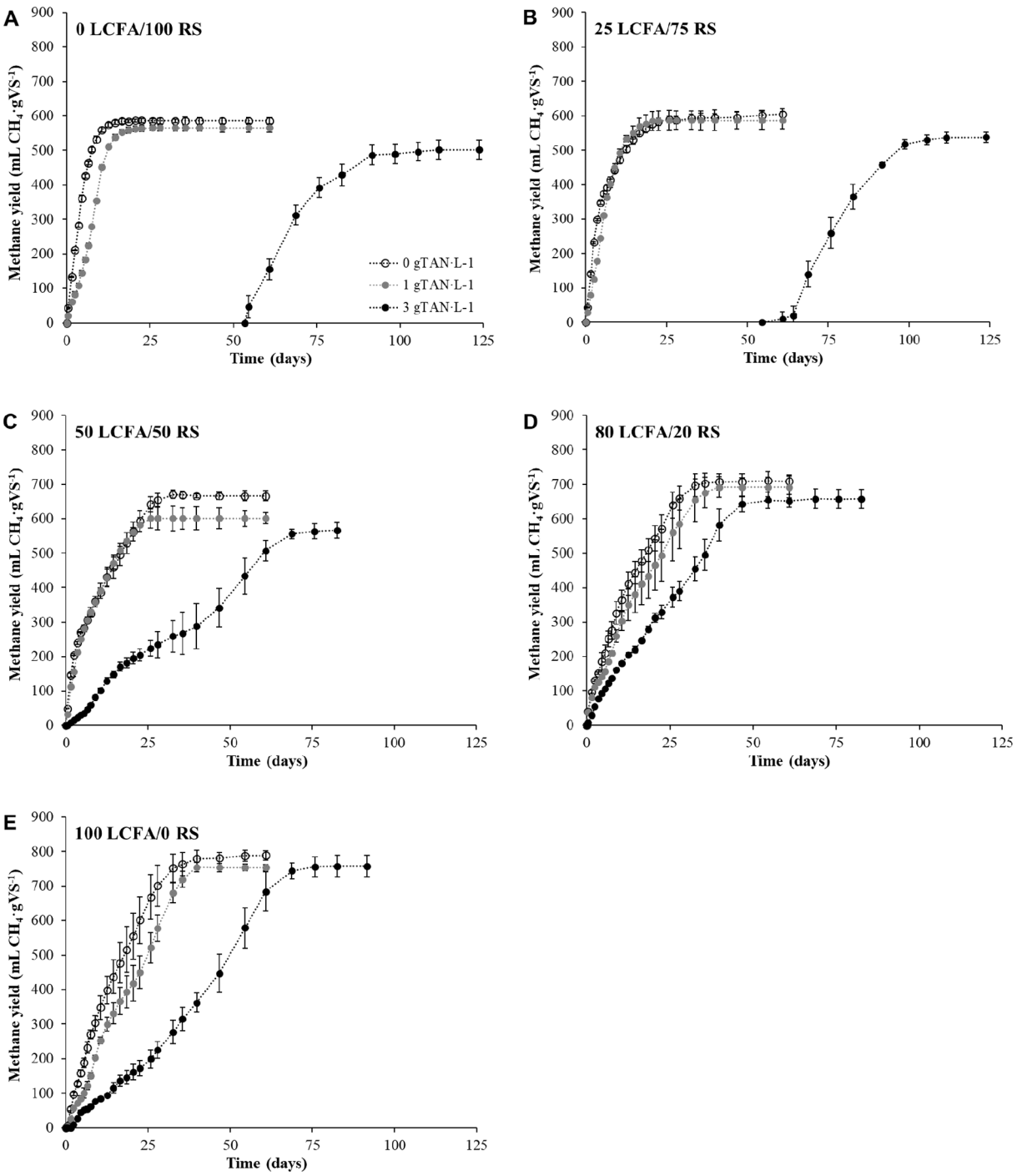

Fig. 3. Cumulative methane yields for the anaerobic mono- and co-digestion batch tests at different TAN concentrations. This figure does not display the 6 $gTAN_{added}·L^{-1}$ results (all tests were completely inhibited) neither negative yields where the blank produced more methane than the test. Error bars show the standard deviation among replicates.

curves can be found in Table S3 and Fig. S2 in the supplementary material. As expected, the model estimated a lower I_N factor (higher inhibition) for the tests carried out at higher TAN concentrations. Model outputs also showed that LCFA could mitigate TAN inhibition since tests with higher LCFA concentration were less inhibited by ammoniacal nitrogen than tests with lower LCFA concentration (brighter area in Fig. 6 bottom right corner). For example, when the TAN concentration was 3 $gTAN_{added}·L^{-1}$, the I_N was 0.06 in the 0 LCFA/100 RS and increased to 0.51 in the 80 LCFA/20 RS.

4. Discussion

4.1. Impact of TAN on the degradation of RS, LCFA and their co-digestion

TAN related inhibition was discarded in the test carried out without TAN addition since NH_3 and NH_4^+ concentrations were far below reported inhibitory values elsewhere (<8 $mgNH_3\text{-}N·L^{-1}$ and <300 $mgTAN·L^{-1}$; Table S2) (Astals et al., 2018; Capson-Tojo et al., 2020; Rajagopal et al., 2013; Yenigün and Demirel, 2013). TAN inhibition was evident in the RS mono-digestion tests (Fig. 3A), where the addition of 1 and 3 $gTAN·L^{-1}$ led to moderate (I_N = 0.57) and severe (I_N = 0.06)

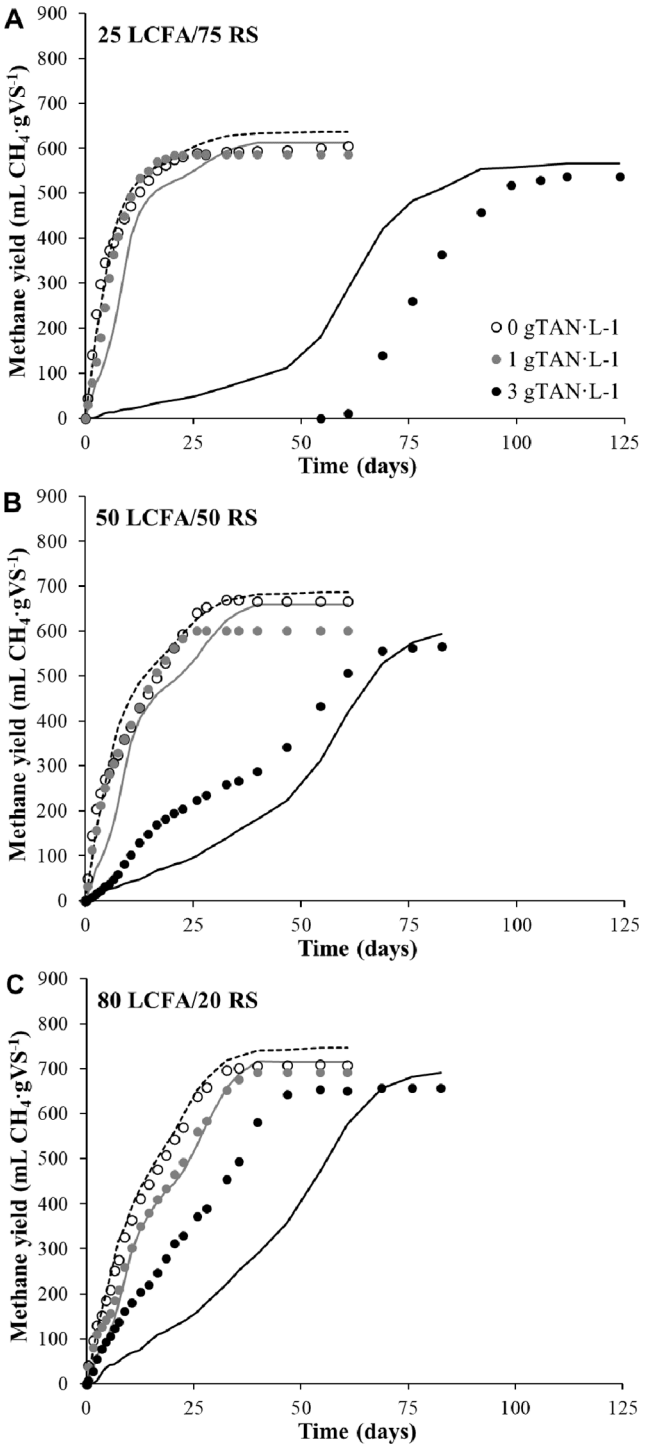

Fig. 4. Comparative of the experimental (dots) and theoretical (lines) methane yields for the co-digestion tests at different TAN concentrations. The theoretical curves were calculated using the mono-digestion results and the amount of RS and LCFA in the mixture.

inhibition of RS degradation, respectively. The severe inhibition noticed in the RS tests at 3 $gTAN_{added}·L^{-1}$ was primarily linked to NH_3 inhibition since the initial and final pH value of the tests was very similar to the control test (0 LCFA/100 RS, 0 $gTAN_{added}·L^{-1}$). Methanogens are more sensitive to TAN inhibition than other trophic groups in AD (Batstone et al., 2002; Rajagopal et al., 2013). Therefore, the most plausible scenario to explain RS severe inhibition at 3 $gTAN_{added}·L^{-1}$ is that the decline of methanogenic activity caused by NH_3, without reducing the

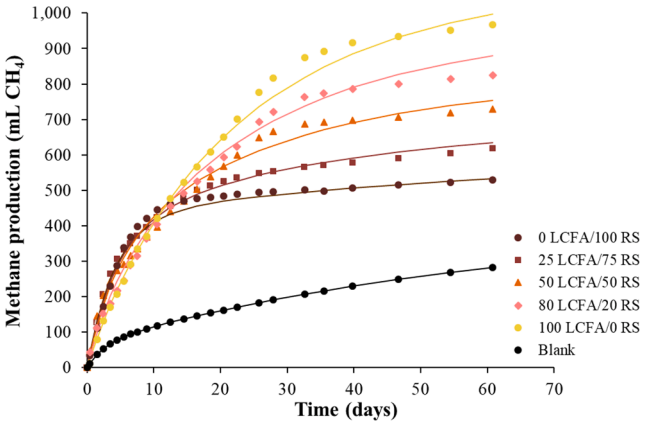

Fig. 5. Experimental (dots) and modelled (lines) cumulative absolute methane production curves at 0 $gTAN_{added}·L^{-1}$.

activity of other anaerobes, resulted in the accumulation of VFA which further inhibited the methanogenic community in a feedback loop that led to process failure. RS had a degradation rate constant of 0.22 day^{-1}, which is higher than that of LCFA (0.05 day^{-1}). It is also likely that the accumulation of VFA was accompanied by a temporary decrease in pH, which could have also contributed to a decreased methanogenic activity. However, the impact of pH on methanogenic activity depends on the sensitivity of methanogens to both pH and NH_3 inhibition since a decrease in pH would also have decreased NH_3 concentration. This suggests that the 50 days lag phase was probably caused by the accumulation of VFA due to NH_3 inhibition. If NH_3 inhibition could be avoided (e.g. with a more resistant archaeal community adapted to NH_3 inhibition), it is likely that the lag phase would have been largely mitigated (Capson-Tojo et al., 2020; Fotidis et al., 2013; Regueiro et al., 2016; Tian et al., 2018). It should be mentioned that the inoculum background concentration was ca. 280 $mgTAN·L^{-1}$. Therefore, the inoculum was not adapted to high TAN concentrations. The inoculum methanogenic community was dominated by *Methanosaeta* (Lu et al., 2018), an acetoclastic methanogen particularly vulnerable to NH_3 inhibition (Capson-Tojo et al., 2020).

Although less pronounced, the impact of TAN inhibition was also evident in the LCFA mono-digestion tests (100 LCFA/0 RS). The addition of 1 and 3 $gTAN·L^{-1}$ led to slight ($I_N = 0.77$) and moderate ($I_N = 0.40$) inhibition of the LCFA degradation, respectively. The lower impact of TAN on LCFA-rich tests could be explained by two distinct hypotheses:

(i) the lower degradation rate of LCFA reduced VFA production and accumulation at the early stages of the batch tests, which prevented inhibition by VFA and pH.
(ii) the adsorption of LCFA on the cell membrane formed a "protective coat" that limited the diffusion of free ammonia into the cell and/or provided a localised lower pH in the vicinity of the microbial cell.

Severe pH inhibition was discarded as main inhibitory mechanism. The maximum pH drop should have been observed in the completely inhibited tests at 6 $gTAN_{added}·L^{-1}$, where the final pH was 5.87–6.05 (see pH values in Table S2). pH values of around 6.0 are not optimal for AD but these values are not low enough to explain the extreme process inhibition (Batstone et al., 2002; Latif et al., 2015). The initial and final pH of the batch tests at 0, 1 and 3 $gTAN_{added}·L^{-1}$ ranged from 7.4 – 6.8 and 6.9–6.7, respectively. These pH values are suitable for AD; however, a temporary pH drop due to a transient VFA accumulation during the batch tests cannot be discarded. Nonetheless, it seems unlikely that pH itself can explain the failure of the 6 $gTAN_{added}·L^{-1}$ tests nor the severe inhibition of the 0 LCFA/100 RS and 25 LCFA/75 RS tests at 3 $gTAN_{added}·L^{-1}$.

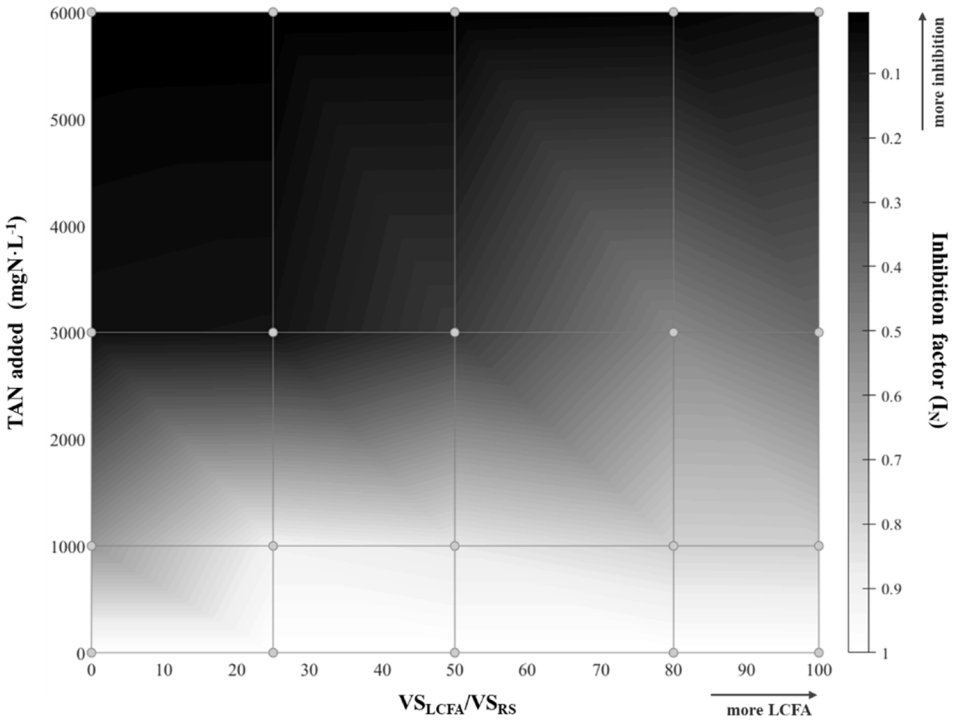

Fig. 6. Ammoniacal nitrogen inhibition factor (I_N) for the mono- and co-digestion tests under study. I_N factor range from 1 (no inhibition, white) to 0 (total inhibition, black). Dots identify the 20 experimental data points.

4.2. TAN and LCFA inhibition interaction

Experimental and modelling results indicate that LCFA mitigate, to a certain degree, TAN inhibition (see Sections 3.2 and 3.3). Besides the comparison between RS and LCFA mono-digestion (see Section 4.1), evidence of LCFA preventing TAN inhibition is found when the 25 LCFA/75 RS and the 50 LCFA/50 RS tests at 3 $gTAN_{added}·L^{-1}$ are compared. These tests had very similar initial characteristics in terms of TAN and pH, and the initial LCFA concentration was below the inhibition onset concentration for LCFA (0.9 and 2.2 $gVS_{LCFA}·L^{-1}$ vs. $KI_{lcfa,min}$ of 4.1 $gVS_{LCFA}·L^{-1}$). Experimental and modelling results support a positive interaction between LCFA and TAN since the 25 LCFA/75 RS test was strongly inhibited ($I_N = 0.07$) while the 50 LCFA/50 RS test was only partly inhibited ($I_N = 0.22$). Besides the lower LCFA concentration, it is worth noting that: (i) the 80 LCFA/20 RS and 100 LCFA/0 RS tests were similarly inhibited at 1 $gTAN_{added}·L^{-1}$ ($I_N = 0.78$ and $I_N = 0.77$, respectively), but the 80 LCFA/20 RS test was notably less inhibited at 3 $gTAN_{added}·L^{-1}$ ($I_N = 0.51$ and $I_N = 0.22$, respectively) and (ii) at 1 $gTAN_{added}·L^{-1}$ the 25 LCFA/75 RS and 50 LCFA/50 RS tests were slightly less inhibited by TAN than the 80 LCFA/20 RS and 100 LCFA/0 RS tests. These results suggest that the interaction between ammoniacal nitrogen and LCFA is not linear, and that it does not only depend on the LCFA concentration.

The current experimental data set does not allow confirmation of the two proposed mechanisms nor elucidates the relative contribution of each mechanism on the positive interaction between TAN and LCFA (see Section 4.1). The partial inhibition of the 0 LCFA/100 RS and 25 LCFA/75 RS tests due to VFA accumulation seems the most plausible explanation since NH_3 and NH_4^+ concentrations were below severe inhibitory concentrations (Capson-Tojo et al., 2020; Fotidis et al., 2013; Rajagopal et al., 2013). The accumulation of VFA and subsequent test inhibition could explain why tests with more RS were more inhibited. However, this hypothesis cannot explain the significant loss of proportionality between the experimental and theoretical plots at 3 $gTAN_{added}·L^{-1}$ (Fig. 4). The fact that the 50 LCFA/50 RS and 80 LCFA/20 RS tests were remarkably less inhibited than expected shows that the test response was not only dependent on the amount of each substrate in the mixture. In this context, it can be hypothesised that the formation of a LCFA layer on the cell membrane could have mitigated ammonia inhibition by (i) limiting the diffusion of NH_3 through the microbial cell membrane and/or (ii) providing a localised lower pH in the vicinity of the microbial cell due to VFA production.

4.3. Future research and industrial implications

This research evaluated the interactions between ammoniacal nitrogen and LCFA inhibition under mesophilic conditions (37 °C). Our results showed an antagonistic co-inhibition effect between both inhibitors (i.e. the combined inhibition effect is lesser than the sum of their individual effect) in contrast to the synergistic co-inhibition (i.e. the combined inhibition effect is greater than the sum of their individual effect) reported by Wang et al. (2016) and Tian et al. (2018) when evaluating the interaction between NH_3 and LCFA under thermophilic conditions. However, mesophilic and thermophilic results cannot be directly compared since temperature significantly affects LCFA solubility and ammoniacal nitrogen fractionation. The lower solubility of LCFA in water at mesophilic conditions makes LCFA less accessible to microorganisms at mesophilic conditions than at thermophilic conditions (Elsamadony et al., 2021). Temperature also affects the TAN acid-base equilibrium constants, with pKa decreasing with temperature. Accordingly, the response of anaerobes, and methanogens in particular, to TAN and LCFA is expected to depend on temperature (Elsamadony et al., 2021; Fotidis et al., 2014; Hwu and Lettinga, 1997; Wang et al., 2016).

Batch tests results are known to be sensitive to the inoculum properties (Holliger et al., 2016; Koch et al., 2017; Mahdy et al., 2017; Raposo et al., 2020). The inoculum used in this study was obtained from a mesophilic anaerobic lagoon operated at a slaughterhouse at ambient temperature (ca. 25 °C). Approximately, one-third of the organic loading rate was biodegradable lipids/LCFA and therefore, the inoculum had the capability to degrade LCFA. On the other hand, the inoculum background NH_4^+ and NH_3 concentrations were relatively low (277 $mgNH_4^+$-N·L^{-1} and 5 $mgNH_3$-N·L^{-1}, respectively) when compared to the

concentrations tested in the study. Tests comparing different inocula (e.g. rich in hydrogenotrophic methanogens) should be carried out to evaluate the relevance of inoculum acclimation to TAN in order to confirm the observed positive interaction between TAN and LCFA under mesophilic conditions. The operation of continuous digesters combined with activity and inhibition tests will provide further insights on the observed positive interaction as well as the relative importance of microbial community acclimation.

The obtained results indicate that using lipid-rich co-substrates could be particularly useful for industrial-scale digesters operated at relatively high TAN concentrations or even to mitigate transient TAN shocks. In such applications, the addition of lipids/LCFA could help to improve process performance by increasing the loading and biogas production rates while partially alleviating TAN inhibition. However, it is important to determine the interaction mechanism between TAN and LCFA and the accompanying inhibitors (pH, H_2 and VFA) prior to scaling up these results to full-scale application. Although pH does not appear to be a major inhibition factor, H_2 might be crucial in systems working at high TAN levels, due to the predominance of hydrogenotrophic methanogenesis and the hydrogenation of unsaturated LCFA (e.g. oleic acid to stearic acid). Finally, it is worth mentioning that improved modelling of LCFA degradation and LCFA inhibition is needed to support these research outcomes.

5. Conclusions

Five slaughterhouse wastewater and LCFA mixtures (100:0, 75:25, 50:50, 20:80, 0:100 on a VS basis) were co-digested at four TAN concentrations (0, 1, 3, 6 $gTAN_{added} \cdot L^{-1}$) to elucidate the interaction between TAN and LCFA inhibition. Experimental and modelling results support the positive interaction between LCFA and TAN since ammoniacal nitrogen inhibition was less severe in LCFA-rich mixtures. Two hypotheses were formulated to describe the observed interaction: (i) the low degradation rate of LCFA prevented the accumulation of VFA at the early stages of the batch, and/or (ii) the formation of a protective-coat mechanism limited the diffusion of ammonia into the cell or provided a localised lower pH in the vicinity of the cell. Further research is needed to confirm these mechanisms and elucidate the relative roles of concomitant inhibitors (VFA, H_2 and pH) in managing inhibition. Overall, these results suggest LCFA do not exacerbate TAN-related inhibition and that LCFA-rich substrates can be utilised as co-substrates in N-rich digesters.

Declaration of Competing Interest

The authors declare that they have no known competing financial interests or personal relationships that could have appeared to influence the work reported in this paper.

Acknowledgments

This research was supported by the Australian Research Council (ARC) DECRA Fellowship (DE170100497) and by the Slovak Grant Agency for Science VEGA (grant 1/0772/16). Dr Chávez-Fuentes academic visit at The University of Queensland was supported by the Mexican National Council of Science and Technology (CONACYT) and by the National Scholarship Programme of the Slovak Republic (NŠP SR). Sergi Astals is grateful to the Spanish Ministry of Science, Innovation and Universities for his Ramon y Cajal fellowship (RYC-2017-22372). Gabriel Capson-Tojo acknowledges the Xunta de Galicia for his postdoctoral fellowship (ED481B-2018/017).

Appendix A. Supplementary material

Supplementary data to this article can be found online at https://doi.org/10.1016/j.wasman.2021.10.015.

References

Angelidaki, I., Alves, M., Bolzonella, D., Borzacconi, L., Campos, J.L., Guwy, A.J., Kalyuzhnyi, S., Jenicek, P., van Lier, J.B., 2009. Defining the biomethane potential (BMP) of solid organic wastes and energy crops: a proposed protocol for batch assays. Water Sci. Technol. 59, 927–934. https://doi.org/10.2166/wst.2009.040.

Angelidaki, I., Ellegaard, L., Ahring, B.K., 1999. A comprehensive model of anaerobic bioconversion of complex substrates to biogas. Biotechnology and Bioengineering 63, 363–372. 10.1002/(SICI)1097-0290(19990505)63:3<363::AID-BIT13>3.0.CO;2-Z.

APHA, 2012. Standard methods for the examination of water and wastewater / American Public Health Association, American Water Works Association, Water Environment Federation, 22nd edition. ed. American Public Health Association (APHA), American Water Works Association (AWWA) and Water Environment Federation (WEF), Washington (D.C.), U.S.

Arnell, M., Astals, S., Åmand, L., Batstone, D.J., Jensen, P.D., Jeppsson, U., 2016. Modelling anaerobic co-digestion in Benchmark Simulation Model No. 2: Parameter estimation, substrate characterisation and plant-wide integration. Water Res. 98, 138–146. https://doi.org/10.1016/j.watres.2016.03.070.

Astals, S., Peces, M., Batstone, D.J., Jensen, P.D., Tait, S., 2018. Characterising and modelling free ammonia and ammonium inhibition in anaerobic systems. Water Res. 143, 127–135. https://doi.org/10.1016/j.watres.2018.06.021.

Batstone, D.J., Keller, J., Angelidaki, I., Kalyuzhnyi, S.V., Pavlostathis, S.G., Rozzi, A., Sanders, W.T., Siegrist, H., Vavilin, V.A., 2002. The IWA Anaerobic Digestion Model No 1 (ADM1). Water Sci. Technol. 45, 65–73. https://doi.org/10.2166/wst.2002.0292.

Capson-Tojo, G., Moscoviz, R., Astals, S., Robles, Á., Steyer, J.-P., 2020. Unraveling the literature chaos around free ammonia inhibition in anaerobic digestion. Renew. Sustain. Energy Rev. 117, 109487 https://doi.org/10.1016/j.rser.2019.109487.

Chen, J.L., Ortiz, R., Steele, T.W.J., Stuckey, D.C., 2014. Toxicants inhibiting anaerobic digestion: A review. Biotechnol. Adv. 32, 1523–1534. https://doi.org/10.1016/j.biotechadv.2014.10.005.

Elsamadony, M., Mostafa, A., Fujii, M., Tawfik, A., Pant, D., 2021. Advances towards understanding long chain fatty acids-induced inhibition and overcoming strategies for efficient anaerobic digestion process. Water Res. 190, 116732 https://doi.org/10.1016/j.watres.2020.116732.

Fernandes, T.V., Keesman, K.J., Zeeman, G., van Lier, J.B., 2012. Effect of ammonia on the anaerobic hydrolysis of cellulose and tributyrin. Biomass Bioenergy 47, 316–323. https://doi.org/10.1016/j.biombioe.2012.09.029.

Fotidis, I.A., Karakashev, D., Angelidaki, I., 2014. The dominant acetate degradation pathway/methanogenic composition in full-scale anaerobic digesters operating under different ammonia levels. Int. J. Environ. Sci. Technol. 11, 2087–2094. https://doi.org/10.1007/s13762-013-0407-9.

Fotidis, I.A., Karakashev, D., Kotsopoulos, T.A., Martzopoulos, G.G., Angelidaki, I., 2013. Effect of ammonium and acetate on methanogenic pathway and methanogenic community composition. FEMS Microbiol. Ecol. 83, 38–48. https://doi.org/10.1111/j.1574-6941.2012.01456.x.

García-Gen, S., Rodríguez, J., Lema, J.M., 2015a. Control strategy for maximum anaerobic co-digestion performance. Water Res. 80, 209–216. https://doi.org/10.1016/j.watres.2015.05.029.

García-Gen, S., Sousbie, P., Rangaraj, G., Lema, J.M., Rodríguez, J., Steyer, J.-P., Torrijos, M., 2015b. Kinetic modelling of anaerobic hydrolysis of solid wastes, including disintegration processes. Waste Manage. 35, 96–104. https://doi.org/10.1016/j.wasman.2014.10.012.

Hagos, K., Zong, J., Li, D., Liu, C., Lu, X., 2017. Anaerobic co-digestion process for biogas production: Progress, challenges and perspectives. Renew. Sustain. Energy Rev. 76, 1485–1496. https://doi.org/10.1016/j.rser.2016.11.184.

Holliger, C., Alves, M., Andrade, D., Angelidaki, I., Astals, S., Baier, U., Bougrier, C., Buffière, P., Carballa, M., de Wilde, V., Ebertseder, F., Fernández, B., Ficara, E., Fotidis, I., Frigon, J.-C., de Laclos, H.F., Ghasimi, D.S.M., Hack, G., Hartel, M., Heerenklage, J., Horvath, I.S., Jenicek, P., Koch, K., Krautwald, J., Lizasoain, J., Liu, J., Mosberger, L., Nistor, M., Oechsner, H., Oliveira, J.V., Paterson, M., Pauss, A., Pommier, S., Porqueddu, I., Raposo, F., Ribeiro, T., Rüsch Pfund, F., Strömberg, S., Torrijos, M., van Eekert, M., van Lier, J., Wedwitschka, H., Wierinck, I., 2016. Towards a standardization of biomethane potential tests. Water Sci. Technol. 74, 2515–2522. https://doi.org/10.2166/wst.2016.336.

Hwu, C.S., Lettinga, G., 1997. Acute toxicity of oleate to acetate-utilizing methanogens in mesophilic and thermophilic anaerobic sludges. Enzyme Microb. Technol. 21, 297–301. https://doi.org/10.1016/S0141-0229(97)00050-1.

Jensen, P.D., Ge, H., Batstone, D.J., 2011. Assessing the role of biochemical methane potential tests in determining anaerobic degradability rate and extent. Water Sci. Technol. 64, 880–886. https://doi.org/10.2166/wst.2011.662.

Kayhanian, M., 1999. Ammonia inhibition in high-solids biogasification: an overview and practical solutions. Environ. Technol. 20, 355–365. https://doi.org/10.1080/09593332008616828.

Koch, K., Lippert, T., Drewes, J.E., 2017. The role of inoculum's origin on the methane yield of different substrates in biochemical methane potential (BMP) tests. Bioresour. Technol. 243, 457–463. https://doi.org/10.1016/j.biortech.2017.06.142.

Latif, M.A., Mehta, C.M., Batstone, D.J., 2015. Low pH anaerobic digestion of waste activated sludge for enhanced phosphorous release. Water Res. 81, 288–293. https://doi.org/10.1016/j.watres.2015.05.062.

Lay, J.J., Li, Y.Y., Noike, T., 1998. The influence of pH and ammonia concentration on the methane production in high-solids digestion processes. Water Environ. Res. 70, 1075–1082. https://doi.org/10.2175/106143098X123426.

Long, J.H., Aziz, T.N., Reyes, F.L. de los, Ducoste, J.J., 2012. Anaerobic co-digestion of fat, oil, and grease (FOG): A review of gas production and process limitations.

Process Safety and Environmental Protection 90, 231–245. 10.1016/j.psep.2011.10.001.

Lu, Y., Liaquat, R., Astals, S., Jensen, P., Batstone, D., Tait, S., 2018. Relationship between microbial community, operational factors and ammonia inhibition resilience in anaerobic digesters at low and moderate ammonia background concentrations. New Biotechnol. 44, 23–30. https://doi.org/10.1016/j.nbt.2018.02.013.

Mahdy, A., Fotidis, I.A., Mancini, E., Ballesteros, M., González-Fernández, C., Angelidaki, I., 2017. Ammonia tolerant inocula provide a good base for anaerobic digestion of microalgae in third generation biogas process. Bioresour. Technol. 225, 272–278. https://doi.org/10.1016/j.biortech.2016.11.086.

Mao, C., Feng, Y., Wang, X., Ren, G., 2015. Review on research achievements of biogas from anaerobic digestion. Renew. Sustain. Energy Rev. 45, 540–555. https://doi.org/10.1016/j.rser.2015.02.032.

Mata-Alvarez, J., Dosta, J., Romero-Güiza, M.S., Fonoll, X., Peces, M., Astals, S., 2014. A critical review on anaerobic co-digestion achievements between 2010 and 2013. Renew. Sustain. Energy Rev. 36, 412–427. https://doi.org/10.1016/j.rser.2014.04.039.

Nghiem, L.D., Koch, K., Bolzonella, D., Drewes, J.E., 2017. Full scale co-digestion of wastewater sludge and food waste: Bottlenecks and possibilities. Renew. Sustain. Energy Rev. 72, 354–362. https://doi.org/10.1016/j.rser.2017.01.062.

Orsavova, J., Misurcova, L., Ambrozova, J., Vicha, R., Mlcek, J., 2015. Fatty acids composition of vegetable oils and its contribution to dietary energy intake and dependence of cardiovascular mortality on dietary intake of fatty acids. Int. J. Mol. Sci. 16, 12871–12890.

Palatsi, J., Viñas, M., Guivernau, M., Fernandez, B., Flotats, X., 2011. Anaerobic digestion of slaughterhouse waste: Main process limitations and microbial community interactions. Bioresour. Technol. 102, 2219–2227. https://doi.org/10.1016/j.biortech.2010.09.121.

Peces, M., Pozo, G., Koch, K., Dosta, J., Astals, S., 2020. Exploring the potential of co-fermenting sewage sludge and lipids in a resource recovery scenario. Bioresour. Technol. 300, 122561 https://doi.org/10.1016/j.biortech.2019.122561.

Pereira, M., Pires, O., Mota, M., Alves, M., 2005. Anaerobic biodegradation of oleic and palmitic acids: evidence of mass transfer limitations caused by long chain fatty acid accumulation onto the anaerobic sludge. Biotechnol. Bioeng. 92, 15–23.

Rajagopal, R., Massé, D.I., Singh, G., 2013. A critical review on inhibition of anaerobic digestion process by excess ammonia. Bioresour. Technol. 143, 632–641. https://doi.org/10.1016/j.biortech.2013.06.030.

Raposo, F., Borja, R., Ibelli-Bianco, C., 2020. Predictive regression models for biochemical methane potential tests of biomass samples: Pitfalls and challenges of laboratory measurements. Renew. Sustain. Energy Rev. 127, 109890 https://doi.org/10.1016/j.rser.2020.109890.

Rasit, N., Idris, A., Harun, R., Wan Ab Karim Ghani, W.A., 2015. Effects of lipid inhibition on biogas production of anaerobic digestion from oily effluents and sludges: An overview. Renewable and Sustainable Energy Reviews 45, 351–358. 10.1016/j.rser.2015.01.066.

Regueiro, L., Carballa, M., Lema, J.M., 2016. Microbiome response to controlled shifts in ammonium and LCFA levels in co-digestion systems. J. Biotechnol. 220, 35–44. https://doi.org/10.1016/j.jbiotec.2016.01.006.

Rodríguez-Méndez, R., Bihan, Y.L., Béline, F., Lessard, P., 2017. Long chain fatty acids (LCFA) evolution for inhibition forecasting during anaerobic treatment of lipid-rich wastes: Case of milk-fed veal slaughterhouse waste. Waste Manage. 67, 51–58. https://doi.org/10.1016/j.wasman.2017.05.028.

Romero-Güiza, M., Mata-Alvarez, J., Chimenos, J., Astals, S., 2016. The effect of magnesium as activator and inhibitor of anaerobic digestion. Waste Manage. 56, 137–142.

Salama, E.-S., Saha, S., Kurade, M.B., Dev, S., Chang, S.W., Jeon, B.-H., 2019. Recent trends in anaerobic co-digestion: Fat, oil, and grease (FOG) for enhanced biomethanation. Prog. Energy Combust. Sci. 70, 22–42. https://doi.org/10.1016/j.pecs.2018.08.002.

Tian, H., Karachalios, P., Angelidaki, I., Fotidis, I.A., 2018. A proposed mechanism for the ammonia-LCFA synergetic co-inhibition effect on anaerobic digestion process. Chem. Eng. J. 349, 574–580.

Wang, H., Fotidis, I.A., Angelidaki, I., 2016. Ammonia–LCFA synergetic co-inhibition effect in manure-based continuous biomethanation process. Bioresour. Technol. 209, 282–289. https://doi.org/10.1016/j.biortech.2016.03.003.

Weinrich, S., Astals, S., Hafner, S.D., Koch, K., 2020. Kinetic modelling of anaerobic batch tests, in: Collection of Methods for Biogas: Methods to Determine Parameters for Analysis Purposes and Parameters That Describe Processes in the Biogas Sector, Biomass Energy Use. DBFZ Deutsches Biomasseforschungszentrum gemeinnützige GmbH.

Xie, S., Hai, F.I., Zhan, X., Guo, W., Ngo, H.H., Price, W.E., Nghiem, L.D., 2016. Anaerobic co-digestion: A critical review of mathematical modelling for performance optimization. Bioresour. Technol. 222, 498–512. https://doi.org/10.1016/j.biortech.2016.10.015.

Yenigün, O., Demirel, B., 2013. Ammonia inhibition in anaerobic digestion: A review. Process Biochem. 48, 901–911. https://doi.org/10.1016/j.procbio.2013.04.012.

Zonta, Z., Alves, M.M., Flotats, X., Palatsi, J., 2013. Modelling inhibitory effects of long chain fatty acids in the anaerobic digestion process. Water Res. 47, 1369–1380. https://doi.org/10.1016/j.watres.2012.12.007.